Intravenous arachnoid granulation volume changes in patients with Parkinson disease

Melanie Leguizamon

Dr. Daniel Claassen & Dr. Elizabeth Catania

PSY 3980

Abstract

We apply novel deep learning algorithms to T2-weighted MRI to test hypotheses regarding arachnoid granulation (AG) hypertrophy in patients with Parkinson's disease (PD). Using this method, we identify AG protruding into the superior sagittal sinus, which may serve as a site of CSF egress. Results from statistical analyses suggest a significant increase in total AG volume in patients with PD compared to age-matched healthy controls, potentially indicating reduced neurofluid clearance efficiency. Further correlational analyses revealed revealed significant relationships between total AG volume and MiniBEST, as well as significant relationships for AG number with MiniBEST and SDMT. Actigraphy data indicate a negative relationship between total AG volume and sleep efficiency and a positive relationship between AG volume and number of awakenings, but no significant relationships with other actigraphy sleep measures. Finally, sleep efficiency was strongly negatively correlated with AG number before correcting for false discovery rate. Chronic sleep disturbance may contribute to AG hypertrophy as a compensatory mechanism for a dysregulated glymphatic system in patients with PD to clear waste.

Introduction

To ensure homeostasis, the brain must have a mechanism by which to clear excess fluid and aggregated solutes associated with pathology and accelerated aging. In neurodegenerative disorders, individuals are plagued by the accumulation of misfolded proteins and an impaired clearance system to rid the brain of these wastes. One system involved in this waste clearance is the glial-lymphatic, or "glymphatic," model, which has been hypothesized to explain the unidirectional influx of cerebrospinal fluid (CSF) into the brain and along perivascular spaces to clear interstitial solutes. Additionally, the meningeal lymphatic vessels aid in further facilitating the outflow of CSF from the central nervous system (CNS) to lymphatic vessels in the body (Bohr et al., 2022). Dysfunction in these systems could thereby contribute to the development and aggravation of disease state, as fewer metabolic wastes are cleared from the brain tissues and CNS. Understanding bulk CSF flow and the

recently proposed glymphatic system is critical to informing the current literature pertaining to the development and progression of neurodegenerative disease.

Although there is no conventional lymphatic system in the brain, like that found in other organs, the brain nevertheless has a system to drain waste out of the CNS space (Gouveia-Freitas & Bastos-Leite, 2021). Crucial to this drainage is CSF, which is produced in and largely secreted from the choroid plexus, a structure composed of epithelial cells in the ventricles of the brain (Khasawneh et al., 2018). CSF flows through the ventricular system until it eventually reaches the subarachnoid space to be reabsorbed into the bloodstream and cervical lymphatics via multiple hypothesized structures, including arachnoid granulations. The functions of CSF include protecting, nourishing, and clearing waste from the brain, which supports the maintenance of a stable environment. If functioning correctly, CSF could therefore aid in the prevention and/or slowing of pathology progression (Telano & Baker, 2022). Further, the composition of CSF changes with both human aging and neurodegenerative disease, either in reduced production or in reduced flow rate, leading to a variety of imbalances in metabolic homeostasis and accumulation of toxic waste (Mehta et al., 2022). Therefore, imaging and assessment of CSF physiology and flow, especially as it operates within the glymphatic system and bulk flow pathways, is important for developing a better understanding of its role in clinical settings.

The glymphatic system, first visualized in 2012, is an organized macroscopic waste clearance system formed by astroglial cells along peri-vascular routes (Iliff et al., 2012). Aquaporin-4 (AQP4) channels, located at the end feet of astrocytes alongside peri-arterial spaces, enable interstitial fluid influx, promoting the clearance of soluble proteins and metabolites from the brain, with efflux to peri-venous spaces through similar astrocyte end feet AQP4 channels (Hablitz & Nedergaard, 2021). In neurodegenerative disorders, one of the most prominent hallmarks of pathology is the accumulation of misfolded proteins, such as Tau and amyloid beta in Alzheimer's disease (AD) and alpha-synuclein in Parkinson disease (PD). Past research has shown that the perivascular pathway of the glymphatic circuit

contributes to the clearance of these interstitial solutes, and deletion of the AQP4 gene implicated in the pathway suppresses the clearance of amyloid beta (Iliff et al., 2012). Additionally, in mouse models of traumatic brain injury (TBI), a risk factor for tau proteinopathy, Iliff et al. (2014) discovered a decrease in glymphatic influx and clearance of interstitial solutes, further promoting tau aggregation associated with later development of dementia and AD. Taken together, these studies demonstrate the potential importance of the glymphatic system in the clearance of toxic waste, with impairment in this system possibly contributing to further neurodegeneration. This supports the present theory that the glymphatic circuit becomes dysfunctional in neurodegenerative disease, leading to the buildup of aberrant proteins and their propagation and further progression of disease state (Lopes et al., 2022).

Parkinson disease, a neurodegenerative disorder characterized by the loss of dopaminergic neurons in the substantia nigra pars compacta, as well as alpha-synuclein and often beta-amyloid proteinopathy, is one such disease state associated with impaired CSF outflow and brain waste clearance. PD is the second most common neurodegenerative disorder and currently has no known cause. It is thought to represent an accelerated pattern of aging that manifests in cognitive, motor, and sleep impairments (Mhyre et al., 2012). While dopaminergic mechanisms underlying PD have been studied, neurofluid circulation impairments, which are more difficult to measure, may also contribute to the development of Parkinson disease and remain understudied.

Attempts to uncover the relationship between protein aggregation and dysfunctional CSF egress have been made in various animal models of PD. For example, Ding et al. (2021) discovered that in patients with idiopathic PD, there is a significant reduction in meningeal lymphatic vessel flow and a delay in deep cervical lymph node perfusion; after injecting alpha-synuclein into mice to overexpress the toxin, there was a similar delay in meningeal lymphatic drainage. Furthermore, Zou et al. (2019) demonstrated that blocking meningeal lymphatic drainage in PD mouse models overexpressing alpha-synuclein exacerbated glymphatic system dysfunction and increased alpha-synuclein aggregation and motor deficits associated with PD. Overall, the findings by Zou and colleagues build upon those by Ding

et al. by demonstrating how manipulating meningeal lymphatic vessel flow affects protein accumulation and waste clearance, just as manipulating abnormal protein concentration negatively influences lymphatic drainage. From these reports, the glymphatic system seems to play a role in PD pathogenesis, and impairment in this system necessitates compensatory mechanisms to further clear waste products.

Besides meningeal lymphatic vessels and other structures potentially involved in CSF regulation and egress, arachnoid granulations (AG) serve as another critical efflux point for CSF, as they allow CSF to flow out in bulk when the glymphatic system becomes dysregulated (Vinje et al., 2020). AGs were first described and dissected in the early 16th century by Antonio Pacchioni, who uncovered their relationship to the sagittal sinus and potential role in brain fluid egress (Brunori et al., 1993). In 1870, Trolard confirmed the hypothesis that AGs represent a hypertrophy of normal arachnoid villi and project into both the lacuna lateralis and the superior sagittal sinus directly (Trolard, 1892). In addition to being larger in size, AGs are more complex than arachnoid villi in that they have endothelial-lined tubules that extend from the subarachnoid space (SAS) to the venous system (Grossman & Potts, 1974). While AGs are not present at birth, villi are found in all human brains and smaller mammal brains before maturation, but they are too microscopic to be seen. By 18 months of age, however, AGs are visible on gross inspection in larger mammals and humans, forming identifiable nodules in the sinus lumen at four years old and continuing to grow in volume and number thereafter (le Gros Clark, 1920).

According to histological evidence, AGs protrude from the arachnoid membrane into the dural venous sinuses. The composition and morphology of AGs are heterogeneous, with five potential types of AG, including intra-sinus (Type I), stromal (Type II), diploic (Type III), epidural (Type IV), and subdural (Type V) (Shah et al., 2023). Across aging, AG diameter, stalk diameter, and number of lobes is positively correlated with age (Hett et al., 2024), while percentage of meningothelial covering of AG is inversely correlated with age (Shah et al., 2023), along with significant changes in the internal milieu of AG over time. It is also suggested that villi develop into AGs due to the pressure of CSF that causes the villi to become distended into the venous lumen cavity. In the present study, only type I AGs were

analyzed, but our future work will expand this definition to include the more recently proposed various types of AG.

In terms of their function, AGs act as one-way valves to allow for unidirectional flow of CSF to exit the subarachnoid space and re-enter venous circulation (Neurosurgery, 2019). AGs are found in approximately 2/3 of the population, most commonly in the transverse sinuses and superior sagittal sinus, close to the superficial veins that drain into the sinus. Often, these arachnoid granulations are incidental findings, but they can also cause sinus obstruction, lead to venous hypertension, and clinically present as headaches. In T_1-weighted magnetic resonance imaging (MRI), AG appear with low signal intensity, whereas in T_2-weighted MRI, they appear with high signal intensity, matching the intensity of CSF (Qaqish, 2020). Knowing this, AG, if large enough, can be clearly visualized using neuroimaging methods.

Attempts to characterize CSF flow as it relates to arachnoid granulations have involved mimicking CSF egress in vitro through performing perfusion runs in physiological and non-physiological directions. To inform the current understanding of CSF egress dynamics, Gryzbowski et al. (2008) demonstrated that CSF flows unidirectionally in vivo, due to the difference in pressure between CSF and venous sinuses that drives CSF egress via AG. As for AG, present work highlights its topographic distribution (Gryzbowski et al. 2007) and evaluation of its volumetrics in healthy individuals (Haybaeck et al. 2008). In rare cases, in which individuals are either asymptomatic (Rodrigues & Santos, 2017) or symptomatic (Lu et al., 2012) upon coming into screening, characterization of AGs within specific brain regions has been achieved. However, while this has successfully ruled out the improper identification of other pathological structures, the clinical significance of these AGs remains unclear, as well as a complete understanding of their relationship to CSF outflow.

On the one hand, it is known that CSF outflow occurs via AG (Vinje et al., 2020), in addition to the glymphatic system, and AG prevalence increases across the lifespan, becoming more concentrated in

the cranial bones as opposed to the dural sinuses in healthy aging (Radôs et al., 2021). However, the present research lacks an understanding of AG metric changes (volume, number, frequency, etc.) with age in both healthy and disease populations, and how these metrics compare across different pathology statuses and with sleep impairments. Importantly, PD symptomatology is associated with chronic sleep impairments, leading to the development of other sleep disorders, as well as motor impairments (Stefani & Högl, 2020). Past research has indicated that poorer sleep quality may result in chronic dysregulation of the CSF outflow pathway, as CSF clearance is more active during sleep (Chong et al., 2022). Given that CSF waste clearance via the glymphatic circuit is often dysregulated in neurodegenerative disorders, sleep could play a critical role in the progression of disease state. Specifically, Wang et al. (2022) found that in patients with PD, sleep disorders were significantly associated with reduced CSF alpha-synuclein, further providing support that decreased sleep efficiency impacts CSF clearance of protein aggregates characterizing PD. Additionally, PD is accompanied by brain atrophy, along with thickening of the arachnoid membrane that results in occlusion and degeneration of the villi. Understanding the link between sleep disturbance and impairments in CSF outflow, as well as changes in AG volumetrics, is therefore critical to understanding how these changes lead to disease progression.

Promising methods of analyzing CSF egress through AG valves have evolved from manual identification in Adobe Photoshop (Gryzbowski et al., 2007) and anatomical study of autopsies (Haybaeck et al., 2008) to various forms of magnetic resonance imaging. One type involves relying on intrathecal administration of a gadolinium tracer to visualize CSF entrance into the brain tissue and exchange with interstitial fluid in T_1-weighted MRI in rodents (Iliff et al., 2014). While fluorescence and laser microscopy, as well as contrast-enhanced neuroimaging has effectively mapped CSF flow in rodents, validly translating this to humans has taken extra effort (Mehta et al., 2022). More recently, these imaging modalities have included MR cisternography and MR myelography for CSF localization and phase-contrast MRI and dynamic PET for understanding CSF flow parameters (Mehta et al., 2022). Specifically, the MR types that can be utilized in both humans and animal models involve T_1-weighted,

FLAIR, and arterial spin-labeled MRI (McKnight et al., 2020). Analysis of T_2 relaxation time and single photon emission computed tomography (CT) further allows for visualization of AG (Lu et al. 2022). Nevertheless, standardization of imaging CSF physiology and flow is challenging, as these range of techniques differ in their accuracy, invasiveness, and more (Mehta et al., 2022). Consequently, increasing the use of CSF neuroimaging and evaluating which methods hold the most clinical relevance and effectiveness in developing treatments will be crucial to better understanding the role of CSF flow in neurodegeneration and healthy aging.

Knowing that AG can clearly be visualized in T_1-weighted and T_2-weighted MRI in humans, Hett et al. (2022) reparametrized MRI methods to assess CSF circulation in the parasagittal dura (PSD) space of human participants. They developed a neural networks deep-learning algorithm to automatically segment PSD and superior sinus to test if PSD space volumetrics relate to CSF flow in the cerebral aqueduct and how these measures change over the lifespan. Successfully quantifying PSD volume non-invasively in vivo in humans via this machine learning method allowed Hett and colleagues to uncover an increase in PSD volume in relation to CSF volume, maximum CSF flow, and normal aging in their sample of 62 participants, ranging from 20 to 83 years old. The values they uncovered provide a helpful normative range of PSD volume changes with bulk CSF flow and age, which will be necessary for comparing these values to those of individuals with neurodegenerative disorders. This novel method also provides exponential potential for the segmentation of other brain structures in vivo using non-invasive MRI procedures to understand how various structures may also be implicated in glymphatics and neurodegeneration.

In our study, we propose to apply novel deep learning algorithms using non-contrasted T2-weighted MRI to evaluate changes in arachnoid granulation metrics in patients with Parkinson's disease (PD) compared to age-matched healthy controls. Our overall goals are to (1) apply the deep learning method developed by Hett et al. (2024) for segmentation of arachnoid granulation volume to test our hypotheses pertaining to differences in AG volume between older individuals diagnosed with PD and healthy individuals and (2) determine significant relationships between changes in AG volumetrics and

motor and cognitive impairments. As an exploratory analysis, we also investigate the relationships between changes in AG measures and sleep dysfunction.

While changes in AG volume have been investigated in normal aging (Hett et al.., 2024), the literature lacks an understanding of how these metrics change in patients with PD, largely because there has not been a technology to reliably segment brain structures in vivo. By developing and validating an automatic method for quantifying AG volume and topography, we address this limitation and provide an avenue to understand the relationships between AG changes in patients with and without PD. If there is a change in AG volume in PD patients compared to age-matched healthy controls, correlating with previously discovered changes in PSD space and CSF egress in healthy and disease state, this may indicate a crucial role of AG in regulating the glymphatic system and CSF dynamics. We also hypothesize that there will be correlations between increased AG total volume in patients with PD with worse scores on motor and sleep assessments, as decreased clearance, possibly leading to AG hypertrophy, results in clinical deficits that characterize PD. Finally, we believe that sleep impairment will be significantly associated with larger AG, since chronic sleep disturbance is known to adversely affect the CSF outflow circuit via the glymphatic system.

Methods

Subjects

All participants completed a 3-Tesla MRI between January 2020 and September 2023 at the Vanderbilt University Medical Center (see Table 1). Participants with PD met established criteria for PD. Participants with a history of cerebrovascular disease, anemia, psychosis, or dementia were excluded from the current study. Clinical history was reviewed by a board-certified Neurologist (DOC; experience = 15 years) and anatomical imaging and angiography by a board-certified neuroradiologist (CDM; experience = 13 years). In our original analyses, we looked at only baseline scans for participants with PD with a sample size of 74 (42 HC and 32 PD). Within the PD cohort, 12 participants were female, and 20 were

male. Moreover, 42 age-matched healthy controls were included in this study, with an average of 64.4 years old and a standard deviation of 9.9 years. In the healthy control cohort, 22 participants were female and 20 were male. The PD cohort was composed of individuals with mostly preserved cognitive function, with an average MoCA score of 24.4.

MRI Acquisition

All participants underwent the same acquisition protocol. Participants were scanned at a 3-Tesla MRI (Philips Medical Systems, Best, The Netherlands) with body coil radiofrequency transmission and phased array 32-channel SENSE reception. The scan protocol included standard anatomical imaging consisting of 3D T_1-weighted magnetization-prepared-rapid-gradient-echo (MPRAGE) echo time = 8.1 ms, repetition time = 3.7 ms, flip angle = 8°, resolution = 1 x 1 x 1 mm. 3D T_2-weighted (sagittal acquisition) volumetric isotropic turbo-spin-echo acquisition (VISTA) sequence was planned along the anterior commissure – posterior commissure line: field-of-view = 250x250x188.8 mm, repetition time = 2,500 ms, echo time = 331 ms, spatial resolution = 0.78x0.78x0.78 mm, and scan duration = 247.5s.

Algorithm

The proposed AG segmentation method is based on a cascaded U-Net model (Ronneberger et al., 2015) with 3D patches as inputs (96x64x64voxels). Deep-learning models were trained using 50 manually delineated scans, segmented from scratch. After applying the deep learning model to the full sample (n=74), the scans were corrected with manual delineation to improve the accuracy of the segmentation of AG.

Image Analysis

AG were manually delineated along the superior sagittal sinus (SSS) under the supervision of a board certified neuroradiologist (experience=13 years). Delineation of prefrontal, frontal, parietal, and

occipital regions were identified on the MNI template and projected to the native space. The prefrontal and frontal regions were distinguished by a plane crossing through the pituitary gland and the rostrum of the corpus callosum, such that the prefrontal region lies ventral and the frontal region dorsal to the plane. The parietal region was delineated from the frontal region using the central sulcus and extends to the parietal-occipital fissure; the occipital region was delineated from the parietal-occipital fissure to the most posterior portion.

Cognitive and Motor Assessments

Patients with PD were assessed for cognitive and motor impairments using MoCA, MiniBESTest, and UPDRS Part III. The MoCA, or Montreal Cognitive Assessment, was originally created to detect mild cognitive impairment (MCI), but it has been used to test for dementia and overall cognitive impairment in a wide range of neurodegenerative disorders. Specifically, a Task Force formed by the Parkinson Study Group Cognitive/Psychiatric Working Group found the MoCA to be the most suitable measure for global cognition (Chou et al., 2010). The MiniBESTest is a shortened version of the BESTest, with 16 items scored to assess dynamic balance during gait and transfer movements, but it has a strong relationship with BESTest scores, demonstrating its effectiveness in measuring balance in PD (Leddy et al., 2011). The Single Digit Modality Test (SDMT) is a cognitive test that assesses processing speed and motor speed (Smith, 1982). Finally, Part III of the UPDRS, or Universal Parkinson Disease Rating Scale, was administered by a neurologist, with the participant in the best medical state. Part III is the motor examination portion of the test (Goetz et al., 2008). All clinical assessments were administered on the day of MRI, and all assessment and image acquisition were done with the patient off medication for a period of 16 hours prior to the examination.

Sleep Assessments

Sleep assessment was conducted using the Patient-Reported Outcomes Measurement Information System (PROMIS).The PROMIS assessment includes 8-item short forms in which patients rate their sleep

quality, satisfaction, and disruptions, as well as effects the next day according to a 5-point Likert scale (Hanish et al., 2017). Sleep-wake related PROMIS short forms for two constructs were employed: sleep disturbance (SD) and sleep-related impairment (SRI). SD assesses perception of sleep quality, sleep depth, and restoration associated with sleep, while SRI focuses on perceptions of alertness, sleepiness, and tiredness during usual waking hours. PROMIS sleep questionnaires were administered on the day of the MRI scan, following standard instructions requesting the participant reflect on the last week of symptoms. While T-scores are available for clinical use, the study relied on raw total scores for analyses.

In addition to self-reported sleep assessment, sleep efficiency was estimated using actigraph units (ActiGraph wGT3X-BT). Sleep efficiency is the ratio of time spent asleep to time spent attempting sleep. For this study, we calculated sleep efficiency percentage by dividing the amount of estimated time spent asleep by the total estimated amount of time in bed, both of which are recorded when wearing the actigraphy device. Actigraphy output variables included in this study were sleep efficiency and wake after sleep onset (in hours/day). We obtained baseline sleep data from 11 participants with PD who wore an actigraphy device ranging from 3 to 82 days ($\mu = 22.9$, Med = 18).

Table 1.

Description of the demographics and brain and CSF volumetrics in PD and controls

	PD	Controls	*p*
Demographics			
Number of scans	32	42	-
Age (year)	67.4 [56-79]	64.4 [50-86]	0.09
Sex (F/M)	12/20	22/20	0.17
Brain volume (in cm^3)			
Intracranial	1434.1 [1167.3-1750.0]	1389.7 [1060.6-1639.6]	0.28
Gray matter	720.0 [582.4-895.0]	706.5 [532.8-845.9]	0.61
White matter	430.9 [323.0-588.8]	422.7 [286.4-561.5]	0.55
CSF volume (in cm^3)			
Total	264.2 [177.3-403.4]	242.5 [144.8-389.5]	0.05
Internal[1]	42.9 [15.8-95.6]	37.8 [16.6-72.8]	0.70
External[2]	219.6 [160.7-331.3]	203.4 [123.3-350.2]	0.07

[1] Internal CSF volume comprises lateral, third, and fourth ventricles

[2] External CSF volume comprises all subarachnoid space and other CSF compartment surrounding brain space.

Description of the demographics and brain (total intracranial volume, gray matter volume, and white matter volume) and cerebrospinal fluid (CSF) volumetrics (total, internal, and external) in patients with Parkinson disease (PD) and controls.

Table 2.

Description of the clinical and sleep assessments conducted in PD

	Mean [min-max]
Disease duration (n=32)	
Years since diagnosis	4.4 [0.1-18]
Years since onset	6.2 [0.4-19]
Clinical Assessments (n=32)	
MoCA	24.4 [18-30]
SDMT	41.6 [24-57]
MiniBEST	21 [3-28]
UPDRS (Part III)	31.3 [8-61]
Self-reported sleep assessments (n=32)	
PROMIS SD	20.3 [9-31]
PROMIS SRI	15.8 [8-28]
Actigraphy (n=14)	
Sleep Efficiency (%)	94.8 [91.6-97.1]
Wake after sleep onset *(minutes/day)*	26.1 [9.6-30.7]

Description of the clinical presentation and sleep assessments conducted on the cohort of patients with Parkinson disease (PD). Clinical assessments were conducted off medication.

Statistical Analysis

Distribution of age and sex ratio differences between healthy control and patients with PD were assessed using Kruskal-Wallis test and Chi-squared test, respectively. Group-wise analysis comparing differences between the two investigated cohorts was performed using a generalized linear model (GLM). AG metrics (i.e., number, total, mean, and maximum AG volume) were used as dependent variables, pathological group (i.e., healthy control and PD) was defined as the independent variable, and age, sex, and intracranial volume (ICV) were used as covariates. Finally, relationships between AG features and clinical (i.e., cognitive and motor) and sleep assessment (self-reported and actigraphy) was determined using

Spearman-rank correlation. All p-values are reported as uncorrected (noted $p_{uncorrected}$) and corrected for false positive rate (noted p_{FDR}).

Results

Demographics and clinical assessments

All participants provided informed, written consent in accordance with the local institutional review board (IRB) and consistent with the Declaration of Helsinki and its amendments. In total, 74 participants were enrolled and scanned in a 3-Tesla MRI. 32 participants were diagnosed with PD (average years of symptoms = 6.2, average years since diagnosis = 4.4). Patients were on average 65.7 years old with a standard deviation of 8.5 years. Within the PD cohort, 12 participants were female, and 20 were male. Moreover, 42 age-matched non-PD controls were included in this study, with an average age of 64.4 years old and a standard deviation of 9.9 years. In the non-PD cohort, 22 participants were female and 20 were male. Details of the clinical and sleep assessments of the PD cohort can be found in Table 1. The PD cohort was composed of individuals with largely preserved cognitive function, with an average MoCA score of 24.4. We obtained baseline sleep data from 14 participants with PD who wore an actigraphy device ranging from 2 to 82 days (average = 23.5 days).

Table 1

Description of demographics and brain and cerebrospinal fluid measures in participants with PD and controls

	PD	Controls	Total	*p*
Demographics				
Number of scans	32	42	74	-
Age (year)	67.4 [56-79]	64.4 [50-86]	65.7 [50-86]	0.09
Sex (F/M)	12/20	22/20	34/40	0.17
Brain Volumetrics				
Intracranial volume (cm^3)	1434.1 [1167.3-1750.0]	1389.7 [1060.6-1639.6]	1405.9 [1060.6-1750.0]	0.28
Gray matter volume (cm^3)	720.0 [582.4-895.0]	706.5 [532.8-845.9]	712.4 [532.8-895.0]	0.61
White matter volume (cm^3)	430.9 [323.0-588.8]	422.7 [286.4-561.5]	426.2 [286.4-588.8]	0.55
CSF Volumetrics				
Cerebrospinal fluid volume (cm^3)	264.2 [177.3-403.4]	242.5 [144.8-389.5]	251.9 [144.8-403.4]	0.05
Internal CSF volume (cm^3)	42.9 [15.8-95.6]	37.8 [16.6-72.8]	40.0 [15.8-95.6]	0.70

External CSF volume (cm^3)	219.6 [160.7-331.3]	203.4 [123.3-350.2]	210.4 [123.3-350.2]	0.07

Description of the demographics and brain (total intracranial volume, gray matter volume, and white matter volume) and cerebrospinal fluid (CSF) volumetrics (total, internal, and external) in patients with Parkinson disease (PD) and controls.

Table 2

Description of clinical and sleep assessments in patients with PD

	Mean [min-max]
Disease duration	
Years since diagnosis	4.4 [0.1-18]
Years since onset	6.2 [0.4-19]
Clinical Assessments	
MoCA	24.4 [18-30]
SDMT	41.6 [24-57]
MiniBEST	21 [3-28]
UPDRS (Part III)	31.3 [8-61]
Self-reported sleep assessments	
PROMIS SD	20.3 [9-31]
PROMIS SRI	15.8 [8-28]
Actigraphy	
Sleep Efficiency (%)	94.8 [91.6-97.1]
Wake after sleep onset *(minutes/day)*	26.1 [9.6-30.7]

Description of the clinical presentation and sleep assessments conducted on the cohort of patients with Parkinson disease (PD). Clinical assessments were conducted off medication.

Group Differences

Spearman correlations (Table 3) revealed a significant relationship between total AG volume in patients with PD and MiniBEST (ρ = 0.48, p_{FDR} = 0.04), but not MoCA (ρ = 0.14, p_{FDR} = 0.61), SDMT (ρ = 0.41, p_{FDR} = 0.10), or UPDRS total score (ρ = -0.02, p_{FDR} = 0.92). We also found significant relationships between AG number in patients with PD with SDMT (ρ = 0.56, p_{FDR} = 0.02) and MiniBEST (ρ = 0.66, p_{FDR}=0.02). We found inconclusive relationships of maximum AG volume in patients with PD with MoCA, SDMT, MiniBEST, and UPDRS total scores (see Table 3).

Figure 1

Examples of intravenous arachnoid granulations in two participants

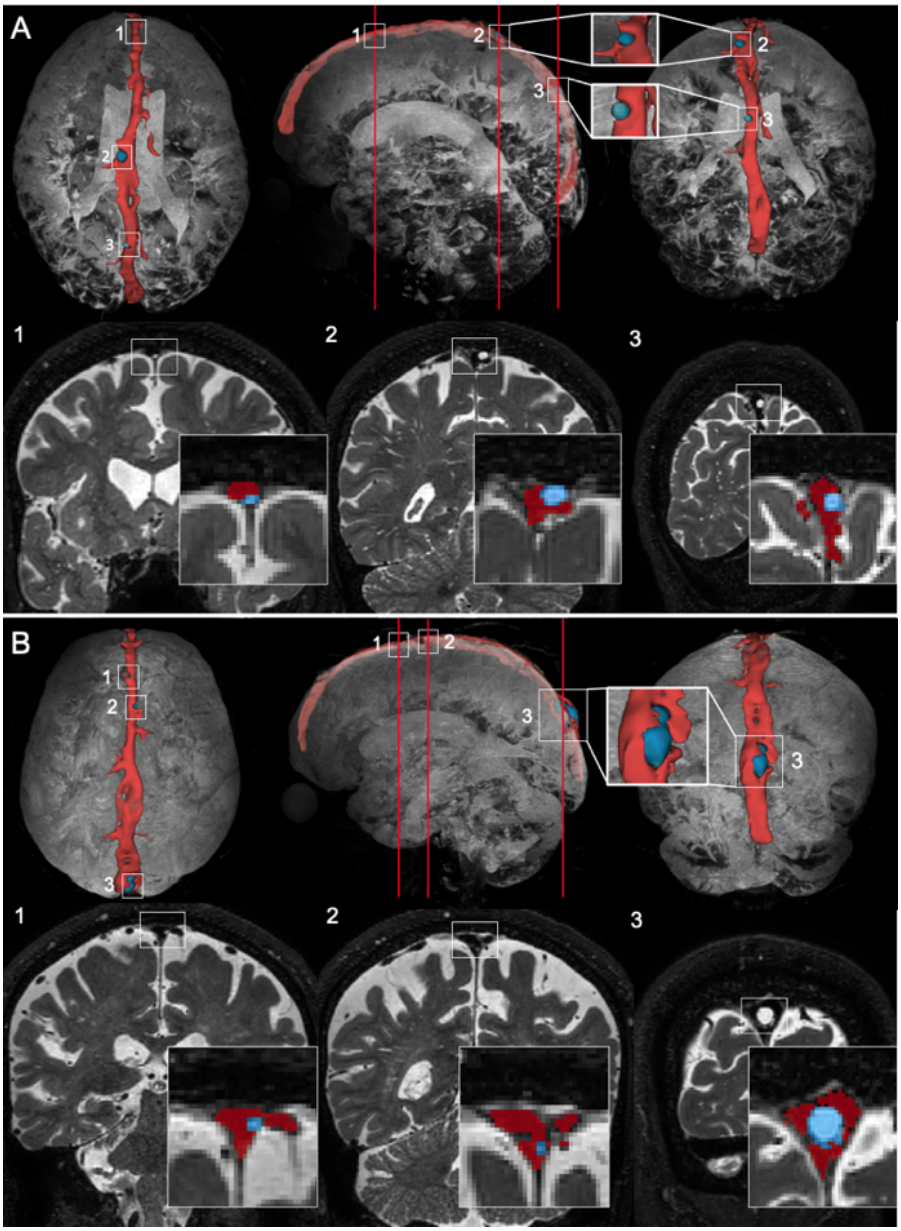

Panels A and B represent the maximum intensity projection (top) and coronal slices (bottom) of T_2-weighted scans, highlighting regions with high concentration of fluids, such as lateral ventricles and subarachnoid space, overlaid with 3D rending of the superior sinus (red), and intravenous arachnoid granulations (blue) from two participants in the axial, sagittal, and coronal planes. Panel A illustrates a participant with increased average AG volume (1, 2, and 3). Panel B illustrates a participant with normal average AG volume (1) and (2), but an increase of maximum AG volume (3). Both participants (Panels A and B) had the same number of detected AG.

Figure 2

Group differences in AG volumetrics between PD and controls

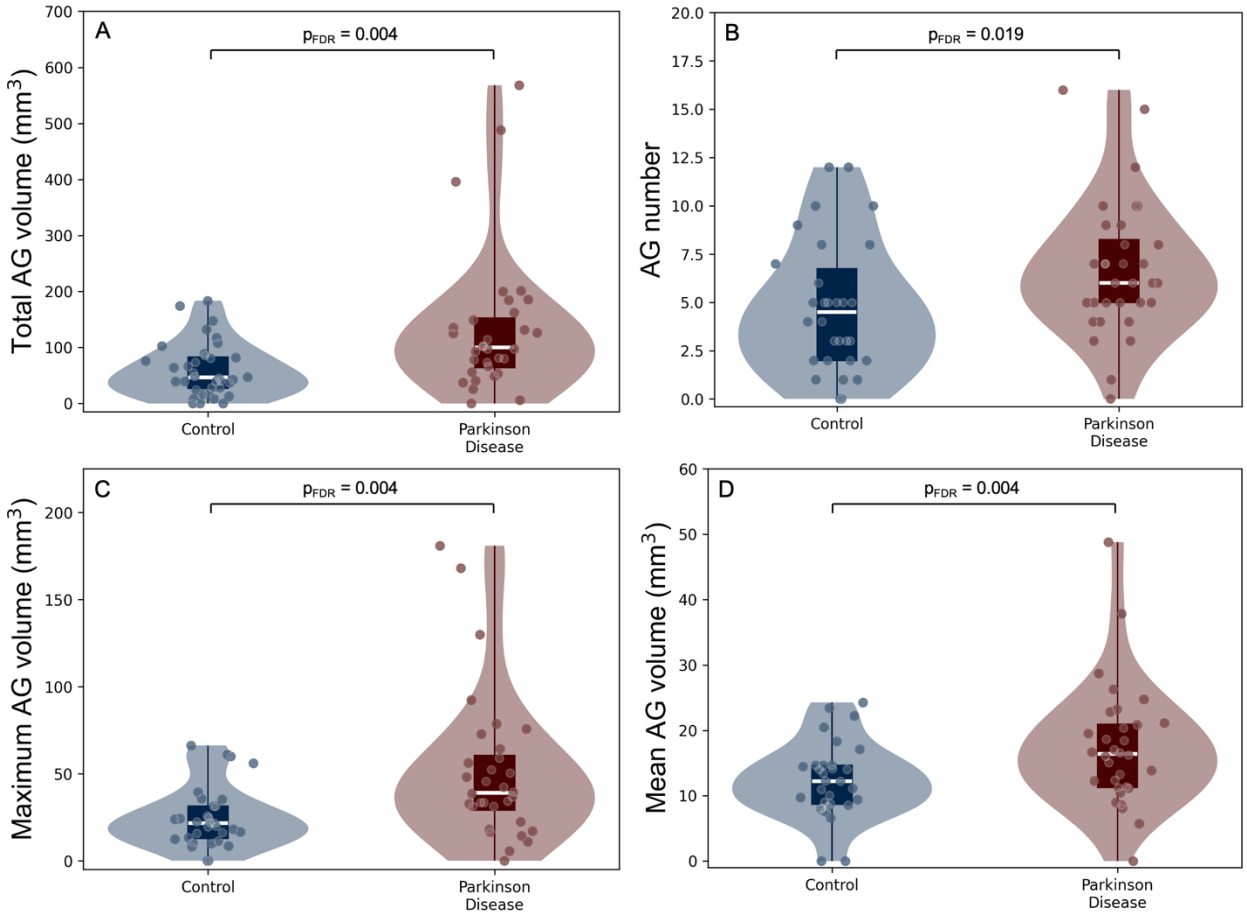

Group differences in arachnoid granulation (AG) total volume (mm^3). Panel A shows significantly increased total AG volume in baseline PD scans compared to HC. Panel B shows significantly increased AG number in PD compared to HC. Panel C shows significantly increased maximum AG volume compared to HC. Panel D shows significantly increased mean AG volume in PD compared to HC.

Correlation with clinical assessments

Spearman correlations (Table 3) revealed a significant relationship between total AG volume in patients with PD and MiniBEST (ρ = 0.48, p_{FDR} = 0.04) and a positive trend between total AG volume and SDMT (ρ = 0.41, p_{raw} = 0.05), but no significant relationships with MoCA (ρ = 0.14, p_{FDR} = 0.61) or UPDRS total score (ρ = -0.02, p_{FDR} = 0.92). We also found significant relationships between AG number in patients with PD with MiniBEST (ρ = 0.66, p_{FDR} = 0.02) and SDMT (ρ = 0.56, p_{FDR} = 0.02). Data suggest

inconclusive relationships of maximum AG volume in patients with PD with MoCA, SDMT, MiniBEST, and UPDRS total scores (Table 3).

Table 3

Correlations between AG measures and clinical assessments in PD

	Total volume			Maximum volume			Mean volume			Number		
	ρ	p_{raw}	p_{FDR}	ρ	p_{raw}	p_{FDR}	ρ	p_{raw}	p_{FDR}	ρ	p_{raw}	p_{FDR}
Cognitive												
MoCA	0.14	0.46	0.61	0.06	0.76	0.89	-0.00	0.98	1.0	0.29	0.11	0.15
SDMT	0.41	0.05	0.10	0.18	0.39	0.78	-0.00	0.98	1.0	**0.56**	**<0.01**	**0.02**
Motor												
UPDRS-III	-0.02	0.92	0.92	0.03	0.89	0.89	0.00	1.0	1.0	-0.00	0.97	0.97
MiniBEST	**0.48**	**0.01**	**0.04**	0.29	0.16	0.64	0.22	0.29	1.0	**0.66**	**<0.01**	**0.02**

Results of Spearman rank correlations between AG measures and clinical assessments (MoCA, MiniBEST, UPDRS) in participants with PD. Significant relationships are underlined and bolded. Underlined refers to significant raw p-values that did not survive False Discovery Rate (FDR) correction. MoCA: Montreal Cognitive Assessment, SDMT: Symbol Digit Modalities Test, UPDRS-III: Universal Parkinson Disease Rating Scale part III, MiniBEST: Mini Balance Evaluation Systems Test.

Correlation with brain and CSF volumetrics

Data indicate no significant relationships between AG metrics and intracranial total volume, grey matter volume, and white matter volume (Supplementary Materials, Table 1). Similarly, data suggest no significant relationships between total, maximum, and mean AG volume and AG number with CSF volumetrics, including total CSF volume, internal CSF volume, and external CSF volume (Supplementary Materials, Table 2).

Correlation with sleep assessments

Table 4 shows details of correlation analyses with sleep assessments. Data suggest inconclusive relationships between AG measures and self-reported sleep assessments, with neither the SD or SRI subscores of the PROMIS measure being significantly related to AG measures, despite showing trends of increased sleep dysfunction (i.e., higher scores on SD and SRI tests) associated with larger AG volumetrics.

Despite not reaching significance, these trends in subjective sleep reports were consistent with findings from actigraphy indicating that increases in AG volume and number in PD are related to sleep dysfunction.

Additionally, all individuals in the PD cohort were asked to wear an actigraphy device for 3 months after MRI acquisition as part of a larger interventional study, but not all participants wore the device for the full duration of the study. Here, we selected a subset of the enrolled PD cohort who wore the actigraph for up to 82 days (range 2 to 82 days) between the MRI acquisition and the beginning of the intervention. This was done to estimate a baseline of sleep parameters using actigraphy that would serve as an exploratory analysis to investigate the relationship between an objective measure of sleep dysfunction (i.e., actigraphy) and AG volumetrics. In participants who wore the actigraphy device (n=14), we noted significant relationships between sleep efficiency and total AG volume (ρ = -0.76, p_{FDR} <0.01). We also found a significant relationship between number of awakenings and total AG volume (ρ = 0.64, p_{FDR} = 0.04).

Further, total CSF volume was significantly related to sleep efficiency (ρ = 0.53, p_{raw} = 0.05) and number of awakenings (ρ = -0.62, p_{raw} = 0.02) before correction for false discovery rate in participants with PD who wore an actigraphy device. Internal and external CSF volume were not significantly related to any sleep assessments. Spearman correlations (Supplementary Materials, Table 3) revealed no significant relationships between brain volumetrics and self-reported sleep assessments and actigraphy measures.

Table 4

Correlations between AG volumetrics and sleep assessments in PD

	Total volume			**Maximum volume**			**Mean volume**			**Number**		
	ρ	p_{raw}	p_{FDR}	ρ	p_{raw}	p_{FDR}	ρ	p_{raw}	p_{FDR}	ρ	p_{raw}	p_{FDR}
Self-reported assessments												
SD	0.25	0.18	0.31	0.22	0.23	0.31	0.14	0.45	0.45	0.34	0.06	0.24
SRI	0.25	0.17	0.39	0.14	0.45	0.45	0.20	0.29	0.39	0.23	0.21	0.39
Actigraphy measures												
SE	**-0.76**	**<0.01**	**<0.01**	-0.50	0.07	0.09	-0.43	0.13	0.13	-0.59	0.03	0.06
WASO	0.46	0.10	0.39	0.21	0.47	0.47	0.35	0.21	0.42	0.27	0.35	0.47
Awak.	**0.64**	**0.01**	**0.04**	0.38	0.19	0.24	0.45	0.11	0.22	0.33	0.24	0.24

Results of Spearman rank correlations between AG measures and sleep assessments (self-reported as well as actigraphy data), in participants with PD. Significant relationships are underlined and bolded. SD: Sleep disturbance, SRI: Sleep related impairment, SE: Sleep efficiency, WASO: Wake after sleep onset.

Discussion

Arachnoid granulation

Intravenous arachnoid granulations have long been observed in the superior sinus lumen (Brunori et al., 1993). Various studies, including both post-mortem (Grzybowski et al., 2007) and in-vivo (Shah et al., 2023) have looked at AG within healthy human control cohorts, and human studies have demonstrated that AGs increase with age in healthy individuals (Kaplanoglu et al., 2023). A previous study has hypothesized that AG hypertrophy results from increased CSF pressure in the subarachnoid space (le Gros Clark, 1920) and/or an impaired glymphatic system (Kress et al., 2014), referring to decreased CSF outflow via the meningeal and cranial nerves. This consequently results in increased CSF pressure and a need for another pathway to rid the brain of metabolic waste, causing AG to hypertrophy to compensate for decreased egress efficiency and aid in further CSF bulk outflow. Other etiologies, such as incidental findings of giant AG (i.e., large enough to fill the dural sinus lumen and cause local dilation) have been reported in patients presenting with venous hypertension and headaches, potentially due to the abnormal growth of AG filling dural sinuses (Kan et al., 2006). In the present study, we observed significantly increased AG volume in patients with PD, in comparison to age-matched healthy controls. We hypothesize that this increase may serve as a compensatory mechanism for impaired CSF clearance via the recently proposed glymphatic pathway, which may jointly occur with further outflow obstruction.

AGs were originally described as a main site for CSF egress (Upton & Weller, 1985). However, studies using intrathecal injection of gadolinium-based contrast agent into CSF challenged this idea (Melin et al., 2023; Rustenhoven et al., 2021), as the contrast agent was reaching maximum concentration in the plasma before peak concentration was detected in peri-sinus structures. This implicated other efflux routes as primary sites for metabolic waste clearance. Although the results of these studies improve the present understanding of CSF egress, there are some limitations that must be addressed.

First, gadolinium-based contrast is known to cross the blood-cerebrospinal fluid barrier and subsequently enter the brain parenchyma (Kanal, 2020). Additionally, there are limitations in equating contrast

movement with fluid and waste movement as the molecular properties of gadolinium-based contrast agent may play a role in distinct egress patterns. Finally, these studies involved injecting tracer into the spinal subarachnoid space, which is inferior and distal to the superior sinus regions, where AG are concentrated. Thus, the tracer may have moved via different egress pathways before ever reaching peri-sinus structures such as AG.

Relationship with brain and CSF volumetrics

Total, maximum, and mean AG volume, as well as AG number, were not significantly correlated with brain or CSF measures, indicating the likelihood that increases in AG volumetrics and count in patients with PD occur independently of global brain atrophy. Past literature has described overall loss of gray matter (Biundo et al., 2011) and ventricular expansion (Mak et al., 2017) in PD compared to controls, but few studies have looked at CSF volumetric changes as they relate to white and gray matter changes in the PD population. Across healthy aging, however, intracranial CSF volume has been shown to increase linearly due to brain volume reduction (Yamada et al., 2023), but whether these changes are replicated in PD remains unknown. Further, the present literature lacks an understanding of how AG volume relates to CSF volume and brain matter volume. Histologic evidence of the composition of AG reports some soft tissue elements with CSF flow turbulence (Mehta et al., 2023), as well as CSF-incongruent fluid (Trimble et al., 2010). As the morphology of AG is not completely understood, these reports reveal a gap in the interpretation of AG structure and function in relation to CSF and brain volumes. Thus, AG hypertrophy in PD compared to controls may reflect a unique difference between these cohorts not otherwise explained by potential changes in CSF or brain volume.

Relationship with clinical assessments

Total AG volume and AG number were significantly correlated with MiniBEST total scores and showed a trend with SDMT scores in patients with PD, despite inconclusive relationships with UPDRS-III scores. This could be due to the fact that the UPDRS-III has limited precision in measuring motor

symptoms in early PD (Regnault et al., 2019), whereas the MiniBEST is considered the strongest individual predictor of falls in patients with PD (Lopes et al., 2020). Therefore, it is possible that the MiniBEST provides a better indication of gait and dynamic instability than the UPDRS-III, as it specifically addresses these motor impairments and UPDRS-III better indicates disease severity. This could mean that changes in AG volumetrics are correlated with the severity of specific balance and postural deficits, rather than more global measures of disease severity. Similarly, total AG volume (before correction for false discovery rate) and AG number were significantly related to scores on the SDMT in patients with PD, but not MoCA, a broader assessment of cognitive functioning. However, since cognitive capacity was largely preserved in our sample, it is likely that only SDMT scores provided enough variability for lower scores to be partially explained by changes in AG volumetrics.

Relationship with the proposed glymphatic system

It should first be noted that this study did not measure perivascular or interstitial flow, which are the fundamental components of the proposed glymphatic system. Results of the experiments conducted in this study could be considered alongside the growing literature investigating changes of glymphatic-related markers in PD, however. Previous studies have implicated the role of the CSF circuits in brain clearance (McKnight et al., 2020) and have suggested glymphatic system dysfunction in patients with PD (Massey et al., 2022; Si et al., 2022; He et al., 2023). By utilizing diffusion tensor imaging (DTI-ALPS) (Taoka et al., 2017; Bae et al., 2023), a coarse metric of perivascular fluid movement at the level of the medullary veins, past research has found a decrease in DTI-ALPS in patients with PD compared to healthy controls (Melin et al., 2023). Additionally, recent work has suggested that fluid movement within the posterior aspects of the suprasellar cistern was reduced in 32 PD relative to 27 non-PD controls (Mays et al., 2023). This suggests decreased fluid motions along the perivascular space of the medullary veins. Further investigations revealed that a lower DTI-ALPS score was positively correlated with disease duration in PD (Ruan et al., 2022), which may reflect downstream dysfunction. In this study, the finding

of increased AG volumetrics in PD compared to controls may serve as a compensatory response to decreased perivascular fluid movement in patients with PD.

Importance of sleep in the CSF circuit

Additionally, past findings have shown the DTI-ALPS index to be significantly lower in individuals with sleep disruption compared to healthy controls (Saito et al., 2023). Recent work has highlighted that the perivascular spaces, which are critical to glymphatic function, are enlarged in chronic sleep deprivation (Adirim et al., 202). The increased volume of perivascular spaces and peri-sinus structures, such as AG, may not only be a marker of aging and neurodegenerative disease, but also of chronic sleep dysfunction. Taken together, these studies lend further support to the suggestion that reduced CSF clearance in both neurodegenerative states and in sleep dysfunctions could contribute to PD pathology progression. As found in our study, total AG volume and AG number (before correction for false discovery rate) significantly relate to sleep efficiency, an objective measure of sleep disturbance. However, this finding was shown in a sample size of 14 participants, and subjective sleep reports (i.e., PROMIS SD and SRI subscores) were not significantly correlated with any changes in AG metrics. Given that the PROMIS is a subjective measure, it is possible that responses from the PD cohort in this study were highly variable and inconsistent with true sleep disturbance. This disturbance may have been more accurately assessed using actigraphy output variables, such as sleep efficiency and number of awakenings, which were both significantly correlated with total AG volume. As total AG volume increases in size, sleep efficiency worsens and number of awakenings increases, aligning with poorer sleep quality either because of or resulting in increases in AG volume.

Clinical significance of the findings

Overall, the data indicate significant increases in total, average, and maximum AG volume, as well as AG number, in a cohort of patients with PD who present with relatively low cognitive impairment. This suggests that cognitive decline might not solely be associated with such enlargement. Data collected provide

support for significant relationships between AG volumetry and various clinical assessment measures (i.e., MiniBEST and SDMT), as well as sleep assessment measures (i.e., actigraphy), potentially implicating a relationship between sleep dysfunction and arachnoid granulation enlargement. To support this hypothesis, increased total AG volume was found to be positive correlated with MiniBEST and SDMT, as well as negatively correlated with actigraphy measure of sleep efficiency and positively correlated with actigraphy measure of number of awakenings.

While results indicate significant relationships between AG hypertrophy and sleep difficulties, future studies are needed to determine the causal mechanism of increased AG volume in PD and its impact on sleep. Potential explanations include AG hypertrophy due to impaired downstream clearance of CSF passage to the dural venous sinuses and/or AG enlargement as a compensatory response to handle increased CSF-mediated waste clearance of protein aggregation in PD pathology. Additionally, as glymphatic clearance is known to occur at higher rates during sleep (Reddy & Van Der Werf, 2020), chronic sleep dysfunction may contribute to a dysregulated glymphatic system and less efficient CSF clearance.

Limitations

Assessing AG structures in MRI

The deep learning algorithm provided a method to automatically segment AG structures in vivo using high resolution 3D T_2-weighted MRI. However, its accuracy can still be improved, and, in this study, manual correction was necessary to ensure a high level of accuracy and precision in delineating AGs. Moreover, despite the use of high-resolution 3D T_2-weighted MRI, the current MRI resolution could only provide visualization of AG volume above 2 mm^3. Therefore, smaller AGs could not be assessed, resulting in a limitation of accurately counting the number of AG protruding the lumen of the superior sinus. To address this limitation, we investigated additional metrics, including total, mean, and maximum AG volume, which rely on larger AG size that allow for better visualization. In this study, we conducted volumetrics analysis of intravenous AG structures. Although volume provides a

comprehensive measure of structural changes, it does not allow us to assess functional changes. Findings presented in this study motivate future functional imaging analysis of AGs to understand the impact of increased AG volume in patients with neurodegenerative proteinopathy.

Potential relationship with sleep dysfunction

Additionally, total AG volume was only significantly correlated with objective measures of sleep from actigraphy but not subjective measures of sleep using self-report PROMIS questionnaires. Further investigation of whether AG volumetrics may relate to various sleep measures in a larger sample and in a controlled setting is necessary to validate the relationships detected in the current study. The present observational study using actigraphy was conducted in a small sample and extracted from a group of individuals who happened to wear an actigraph pre-intervention; as such, the study our data was taken from had not been designed for the purpose of investigating sleep quality in individuals with PD at baseline. Nevertheless, our finding of sleep dysfunction in PD relating to AG hypertrophy motivates further study in a research setting designed and aimed to specifically investigate the relationship between the CSF flow circuit and sleep dysfunction in humans, in both healthy and disease states.

Conclusion

In conclusion, we observed increased volume of intravenous arachnoid granulations in patients with Parkinson disease. AG hypertrophy was also significantly related to motor impairment (on MiniBEST) and revealed trends with poorer cognitive functioning (on SDMT). In our small sample, data revealed a significant relationship between AG volume and sleep dysfunction, potentially suggesting a critical role of sleep in neurofluid regulation. Follow-up studies should investigate the causal role of arachnoid granulations in pathology progression, as well as how impaired sleep may influence this relationship.

References

Aarsland, D., Creese, B., Politis, M., Chaudhuri, K. R., Ffytche, D. H., Weintraub, D., & Ballard, C. (2017). Cognitive decline in Parkinson disease. *Nature Reviews Neurology*, *13*(4), 217–231. https://doi.org/10.1038/nrneurol.2017.27

Adirim, Z. L., Heyn, C., & Murray, B. J. (2023). Sleep and perivascular disruption: An illustrative case of severe sleep apnea, an enlarged Virchow-Robin space, and contralateral asymmetric periodic limb movements. *Sleep Medicine*, *112*, 191–193. https://doi.org/10.1016/j.sleep.2023.10.026

Bae, Y. J., Kim, J.-M., Choi, B. S., Choi, J.-H., Ryoo, N., Song, Y. S., Cho, S. J., & Kim, J. H. (2023). Glymphatic function assessment in Parkinson's disease using diffusion tensor image analysis along the perivascular space. *Parkinsonism & Related Disorders*, *114*, 105767. https://doi.org/10.1016/j.parkreldis.2023.105767

Biundo, R., Formento-Dojot, P., Facchini, S., Vallelunga, A., Ghezzo, L., Foscolo, L., Meneghello, F., & Antonini, A. (2011). Brain volume changes in Parkinson's disease and their relationship with cognitive and behavioural abnormalities. *Journal of the Neurological Sciences*, *310*(1–2), 64–69. https://doi.org/10.1016/j.jns.2011.08.001

Bohr, T., Hjorth, P. G., Holst, S. C., Hrabětová, S., Kiviniemi, V., Lilius, T., Lundgaard, I., Mardal, K.-A., Martens, E. A., Mori, Y., Nägerl, U. V., Nicholson, C., Tannenbaum, A., Thomas, J. H., Tithof, J., Benveniste, H., Iliff, J. J., Kelley, D. H., & Nedergaard, M. (2022). The glymphatic system: Current understanding and modeling. *iScience*, *25*(9), 104987. https://doi.org/10.1016/j.isci.2022.104987

Brunori, A., Vagnozzi, R., & Giuffrè, R. (1993). Antonio Pacchioni (1665–1726): Early studies of the dura mater. *Journal of Neurosurgery*, *78*(3), 515–518. https://doi.org/10.3171/jns.1993.78.3.0515

Chong, P. L. H., Garic, D., Shen, M. D., Lundgaard, I., & Schwichtenberg, A. J. (2022). Sleep, cerebrospinal fluid, and the glymphatic system: A systematic review. *Sleep Medicine Reviews*, *61*, 101572. https://doi.org/10.1016/j.smrv.2021.101572

Chou, K. L., Amick, M. M., Brandt, J., Camicioli, R., Frei, K., Gitelman, D., Goldman, J., Growdon, J., Hurtig, H. I., Levin, B., Litvan, I., Marsh, L., Simuni, T., Tröster, A. I., Uc, E. Y., & on behalf of the Parkinson Study Group Cognitive/Psychiatric Working Group. (2010). A recommended scale for cognitive screening in clinical trials of Parkinson's disease: Cognitive Screening in PD Clinical Trials. *Movement Disorders*, *25*(15), 2501–2507. https://doi.org/10.1002/mds.23362

Department of Radiology, University of Health Sciences, Ataturk Sanatory Training and Research Hospital, Ankara, Turkey, Kaplanoglu, V., Kaplanoglu, H., Department of Radiology, Health Sciences University Diskapi Yildirim Beyazit Training and Research Hospital, Ankara, Turkiye, Turan, A., Department of Radiology, Health Sciences University Diskapi Yildirim Beyazit Training and Research Hospital, Ankara, Turkiye, Dilli, A., & Department of Radiology, Health Sciences University Diskapi Yildirim Beyazit Training and Research Hospital, Ankara, Turkiye. (2023). Evaluation of Arachnoid Granulations in Cranial Dural Sinuses with Contrast-Enhanced 3-Dimensional T1-Weighted Magnetic Resonance Imaging. *Eurasian Journal of Medicine*, *55*(2), 95–99. https://doi.org/10.5152/eurasianjmed.2023.22104

Ding, X.-B., Wang, X.-X., Xia, D.-H., Tian, H.-Y., Fu, Y., Chen, Y.-K., Qin, C., Wang, J.-Q., Xiang, Z., Zhang, Z.-X., Cao, Q.-C., Wang, W., Li, J.-Y., Wu, E., Tang, B.-S., Ma, M.-M., Teng, J.-F., & Wang, X.-J. (2021). Impaired meningeal lymphatic drainage in patients with idiopathic Parkinson's disease. *Nature Medicine*, *27*(3), 411–418. https://doi.org/10.1038/s41591-020-01198-1

Eide, P. K., & Ringstad, G. (2019). Delayed clearance of cerebrospinal fluid tracer from entorhinal cortex in idiopathic normal pressure hydrocephalus: A glymphatic magnetic resonance imaging study. *Journal of Cerebral Blood Flow & Metabolism*, *39*(7), 1355–1368. https://doi.org/10.1177/0271678X18760974

Goetz, C. G., Tilley, B. C., Shaftman, S. R., Stebbins, G. T., Fahn, S., Martinez-Martin, P., Poewe, W., Sampaio, C., Stern, M. B., Dodel, R., Dubois, B., Holloway, R., Jankovic, J., Kulisevsky, J., Lang, A. E., Lees, A., Leurgans, S., LeWitt, P. A., Nyenhuis, D., … LaPelle, N. (2008).

Movement Disorder Society-sponsored revision of the Unified Parkinson's Disease Rating Scale (MDS-UPDRS): Scale presentation and clinimetric testing results: MDS-UPDRS: Clinimetric Assessment. *Movement Disorders*, *23*(15), 2129–2170. https://doi.org/10.1002/mds.22340

Gouveia-Freitas, K., & Bastos-Leite, A. J. (2021). Perivascular spaces and brain waste clearance systems: Relevance for neurodegenerative and cerebrovascular pathology. *Neuroradiology*, *63*(10), 1581–1597. https://doi.org/10.1007/s00234-021-02718-7

Grossman, C. B., & Potts, D. G. (1974). Arachnoid Granulations: Radiology and Anatomy. *Radiology*, *113*(1), 95–100. https://doi.org/10.1148/113.1.95

Grzybowski, D. M., Herderick, E. E., Kapoor, K. G., Holman, D. W., & Katz, S. E. (2007). Human arachnoid granulations Part I: A technique for quantifying area and distribution on the superior surface of the cerebral cortex. *Cerebrospinal Fluid Research*, *4*(1), 6. https://doi.org/10.1186/1743-8454-4-6

Grzybowski, D. M., Holman, D. W., Katz, S. E., & Lubow, M. (2006). In Vitro Model of Cerebrospinal Fluid Outflow through Human Arachnoid Granulations. *Investigative Opthalmology & Visual Science*, *47*(8), 3664. https://doi.org/10.1167/iovs.05-0929

Hablitz, L. M., & Nedergaard, M. (2021). The Glymphatic System: A Novel Component of Fundamental Neurobiology. *The Journal of Neuroscience*, *41*(37), 7698–7711. https://doi.org/10.1523/JNEUROSCI.0619-21.2021

Hanish, A. E., Lin-Dyken, D. C., & Han, J. C. (2017). PROMIS Sleep Disturbance and Sleep-Related Impairment in Adolescents: Examining Psychometrics Using Self-Report and Actigraphy. *Nursing Research*, *66*(3), 246–251. https://doi.org/10.1097/NNR.0000000000000217

Haybaeck, J., Silye, R., & Soffer, D. (2008). Dural arachnoid granulations and "giant" arachnoid granulations. *Surgical and Radiologic Anatomy*, *30*(5), 417–421. https://doi.org/10.1007/s00276-008-0345-2

He, P., Shi, L., Li, Y., Duan, Q., Qiu, Y., Feng, S., Gao, Y., Luo, Y., Ma, G., Zhang, Y., Wang, L., & Nie, K. (2023). The Association of the Glymphatic Function with Parkinson's Disease Symptoms:

Neuroimaging Evidence from Longitudinal and Cross-Sectional Studies. *Annals of Neurology*, *94*(4), 672–683. https://doi.org/10.1002/ana.26729

Hett, K., McKnight, C. D., Eisma, J. J., Elenberger, J., Lindsey, J. S., Considine, C. M., Claassen, D. O., & Donahue, M. J. (2022). Parasagittal dural space and cerebrospinal fluid (CSF) flow across the lifespan in healthy adults. *Fluids and Barriers of the CNS*, *19*(1), 24. https://doi.org/10.1186/s12987-022-00320-4

Bohr, T., Hjorth, P. G., Holst, S. C., Hrabětová, S., Kiviniemi, V., Lilius, T., Lundgaard, I., Mardal, K.-A., Martens, E. A., Mori, Y., Nägerl, U. V., Nicholson, C., Tannenbaum, A., Thomas, J. H., Tithof, J., Benveniste, H., Iliff, J. J., Kelley, D. H., & Nedergaard, M. (2022). The glymphatic system: Current understanding and modeling. *iScience*, *25*(9), 104987. https://doi.org/10.1016/j.isci.2022.104987

Iliff, J. J., Chen, M. J., Plog, B. A., Zeppenfeld, D. M., Soltero, M., Yang, L., Singh, I., Deane, R., & Nedergaard, M. (2014). Impairment of Glymphatic Pathway Function Promotes Tau Pathology after Traumatic Brain Injury. *The Journal of Neuroscience*, *34*(49), 16180–16193. https://doi.org/10.1523/JNEUROSCI.3020-14.2014

Iliff, J. J., Wang, M., Liao, Y., Plogg, B. A., Peng, W., Gundersen, G. A., Benveniste, H., Vates, G. E., Deane, R., Goldman, S. A., Nagelhus, E. A., & Nedergaard, M. (2012). A Paravascular Pathway Facilitates CSF Flow Through the Brain Parenchyma and the Clearance of Interstitial Solutes, Including Amyloid β. *Science Translational Medicine*, *4*(147). https://doi.org/10.1126/scitranslmed.3003748

Kan, P., Stevens, E. A., & Couldwell, W. T. (2006). Incidental giant arachnoid granulation. *AJNR. American Journal of Neuroradiology*, *27*(7), 1491–1492.

Kanal, E. (2020). Intracranial Gadolinium Retention: "Nothing More to See Here… Move Along…." *Radiology*, *294*(2), 386–387. https://doi.org/10.1148/radiol.2019192315

Khasawneh, A., Garling, R., & Harris, C. (2018). Cerebrospinal fluid circulation: What do we know and how do we know it? *Brain Circulation*, *4*(1), 14. https://doi.org/10.4103/bc.BC_3_18

Kress, B. T., Iliff, J. J., Xia, M., Wang, M., Wei, H. S., Zeppenfeld, D., Xie, L., Kang, H., Xu, Q., Liew, J. A., Plog, B. A., Ding, F., Deane, R., & Nedergaard, M. (2014). Impairment of paravascular clearance pathways in the aging brain: Paravascular Clearance. *Annals of Neurology*, *76*(6), 845–861. https://doi.org/10.1002/ana.24271

le Gros Clark, W. E. (1920). On the Pacchionian Bodies. *Journal of Anatomy*, *55*(Pt 1), 40–48.

Leddy, A. L., Crowner, B. E., & Earhart, G. M. (2011). Utility of the Mini-BESTest, BESTest, and BESTest Sections for Balance Assessments in Individuals With Parkinson Disease. *Journal of Neurologic Physical Therapy*, *35*(2), 90–97. https://doi.org/10.1097/NPT.0b013e31821a620c

Lopes, D. M., Llewellyn, S. K., & Harrison, I. F. (2022). Propagation of tau and α-synuclein in the brain: Therapeutic potential of the glymphatic system. *Translational Neurodegeneration*, *11*(1), 19. https://doi.org/10.1186/s40035-022-00293-2

Lu, C.-X. (2012). Multiple occipital defects caused by arachnoid granulations: Emphasis on T2 mapping. *World Journal of Radiology*, *4*(7), 341. https://doi.org/10.4329/wjr.v4.i7.341

Mak, E., Su, L., Williams, G. B., Firbank, M. J., Lawson, R. A., Yarnall, A. J., Duncan, G. W., Mollenhauer, B., Owen, A. M., Khoo, T. K., Brooks, D. J., Rowe, J. B., Barker, R. A., Burn, D. J., & O'Brien, J. T. (2017). Longitudinal whole-brain atrophy and ventricular enlargement in nondemented Parkinson's disease. *Neurobiology of Aging*, *55*, 78–90. https://doi.org/10.1016/j.neurobiolaging.2017.03.012

Massey, A., Boag, M., Magnier, A., Bispo, D., Khoo, T., & Pountney, D. (2022). Glymphatic System Dysfunction and Sleep Disturbance May Contribute to the Pathogenesis and Progression of Parkinson's Disease. *International Journal of Molecular Sciences*, *23*(21), 12928. https://doi.org/10.3390/ijms232112928

Mays, G. P., Hett, K., Eisma, J. J., McKnight, C. D., Elenberger, J., Song, A. K., Considine, C. M., Han, C., Claassen, D. O., & Donahue, M. J. (2023, June 8). *DWI with dynamic b-value cycling reveals*

evidence of reduced suprasellar cistern neurofluid motion in Parkinson's disease. The International Society of Magnetic Resonance in Medicine (ISMRM), Toronto, CA.

McKnight, C. D., Rouleau, R. M., Donahue, M. J., & Claassen, D. O. (2020). The Regulation of Cerebral Spinal Fluid Flow and Its Relevance to the Glymphatic System. *Current Neurology and Neuroscience Reports*, *20*(12), 58. https://doi.org/10.1007/s11910-020-01077-9

Mehta, N. H., Suss, R. A., Dyke, J. P., Theise, N. D., Chiang, G. C., Strauss, S., Saint-Louis, L., Li, Y., Pahlajani, S., Babaria, V., Glodzik, L., Carare, R. O., & de Leon, M. J. (2022). Quantifying cerebrospinal fluid dynamics: A review of human neuroimaging contributions to CSF physiology and neurodegenerative disease. *Neurobiology of Disease*, *170*, 105776. https://doi.org/10.1016/j.nbd.2022.105776

Melin, E., Ringstad, G., Valnes, L. M., & Eide, P. K. (2023). Human parasagittal dura is a potential neuroimmune interface. *Communications Biology*, *6*(1), 260. https://doi.org/10.1038/s42003-023-04634-3

Mhyre, T. R., Boyd, J. T., Hamill, R. W., & Maguire-Zeiss, K. A. (2012). Parkinson's Disease. In J. R. Harris (Ed.), *Protein Aggregation and Fibrillogenesis in Cerebral and Systemic Amyloid Disease* (Vol. 65, pp. 389–455). Springer Netherlands. https://doi.org/10.1007/978-94-007-5416-4_16

Qaqish, N. (2020). Arachnoid granulation. In *Radiopaedia.org*. Radiopaedia.org. https://doi.org/10.53347/rID-84682

Radoš, M., Živko, M., Periša, A., Orešković, D., & Klarica, M. (2021). No Arachnoid Granulations—No Problems: Number, Size, and Distribution of Arachnoid Granulations From Birth to 80 Years of Age. *Frontiers in Aging Neuroscience*, *13*, 698865. https://doi.org/10.3389/fnagi.2021.698865

Reddy, O. C., & Van Der Werf, Y. D. (2020). The Sleeping Brain: Harnessing the Power of the Glymphatic System through Lifestyle Choices. *Brain Sciences*, *10*(11), 868. https://doi.org/10.3390/brainsci10110868

Regnault, A., Boroojerdi, B., Meunier, J., Bani, M., Morel, T., & Cano, S. (2019). Does the MDS-UPDRS provide the precision to assess progression in early Parkinson's disease? Learnings from

the Parkinson's progression marker initiative cohort. *Journal of Neurology*, *266*(8), 1927–1936. https://doi.org/10.1007/s00415-019-09348-3

Ringstad, G., Valnes, L. M., Dale, A. M., Pripp, A. H., Vatnehol, S.-A. S., Emblem, K. E., Mardal, K.-A., & Eide, P. K. (2018). Brain-wide glymphatic enhancement and clearance in humans assessed with MRI. *JCI Insight*, *3*(13), e121537. https://doi.org/10.1172/jci.insight.121537

Rodrigues, J. R., & Santos, G. R. (2017). Brain Herniation into Giant Arachnoid Granulation: An Unusual Case. *Case Reports in Radiology*, *2017*, 1–4. https://doi.org/10.1155/2017/8532074

Ronneberger, O., Fischer, P., & Brox, T. (2015). U-Net: Convolutional Networks for Biomedical Image Segmentation. In N. Navab, J. Hornegger, W. M. Wells, & A. F. Frangi (Eds.), *Medical Image Computing and Computer-Assisted Intervention – MICCAI 2015* (Vol. 9351, pp. 234–241). Springer International Publishing. https://doi.org/10.1007/978-3-319-24574-4_28

Ruan, X., Huang, X., Li, Y., Li, E., Li, M., & Wei, X. (2022). Diffusion Tensor Imaging Analysis Along the Perivascular Space Index in Primary Parkinson's Disease Patients With and Without Freezing of Gait. *Neuroscience*, *506*, 51–57. https://doi.org/10.1016/j.neuroscience.2022.10.013

Rustenhoven, J., Drieu, A., Mamuladze, T., De Lima, K. A., Dykstra, T., Wall, M., Papadopoulos, Z., Kanamori, M., Salvador, A. F., Baker, W., Lemieux, M., Da Mesquita, S., Cugurra, A., Fitzpatrick, J., Sviben, S., Kossina, R., Bayguinov, P., Townsend, R. R., Zhang, Q., … Kipnis, J. (2021). Functional characterization of the dural sinuses as a neuroimmune interface. *Cell*, *184*(4), 1000-1016.e27. https://doi.org/10.1016/j.cell.2020.12.040

Saito, Y., Hayakawa, Y., Kamagata, K., Kikuta, J., Mita, T., Andica, C., Taoka, T., Uchida, W., Takabayashi, K., Tuerxun, R., Mahemuti, Z., Yoshida, S., Kitagawa, T., Arai, T., Suzuki, A., Sato, K., Nishizawa, M., Akashi, T., Shimoji, K., … Aoki, S. (2023). Glymphatic system impairment in sleep disruption: Diffusion tensor image analysis along the perivascular space (DTI-ALPS). *Japanese Journal of Radiology*. https://doi.org/10.1007/s11604-023-01463-6

Shah, T., Leurgans, S. E., Mehta, R. I., Yang, J., Galloway, C. A., De Mesy Bentley, K. L., Schneider, J. A., & Mehta, R. I. (2023). Arachnoid granulations are lymphatic conduits that communicate with

bone marrow and dura-arachnoid stroma. *Journal of Experimental Medicine*, *220*(2), e20220618. https://doi.org/10.1084/jem.20220618

Si, X., Guo, T., Wang, Z., Fang, Y., Gu, L., Cao, L., Yang, W., Gao, T., Song, Z., Tian, J., Yin, X., Guan, X., Zhou, C., Wu, J., Bai, X., Liu, X., Zhao, G., Zhang, M., Pu, J., & Zhang, B. (2022). Neuroimaging evidence of glymphatic system dysfunction in possible REM sleep behavior disorder and Parkinson's disease. *Npj Parkinson's Disease*, *8*(1), 54. https://doi.org/10.1038/s41531-022-00316-9

Smith, A. (1982). Symbol Digit Modalities Test (SDMT). Manual (Revised). *Los Angeles: Western Psychological Services*.

Stefani, A., & Högl, B. (2020). Sleep in Parkinson's disease. *Neuropsychopharmacology*, *45*(1), 121–128. https://doi.org/10.1038/s41386-019-0448-y

Taoka, T., Masutani, Y., Kawai, H., Nakane, T., Matsuoka, K., Yasuno, F., Kishimoto, T., & Naganawa, S. (2017). Evaluation of glymphatic system activity with the diffusion MR technique: Diffusion tensor image analysis along the perivascular space (DTI-ALPS) in Alzheimer's disease cases. *Japanese Journal of Radiology*, *35*(4), 172–178. https://doi.org/10.1007/s11604-017-0617-z

Telano, L. N., & Baker, S. (2018). Physiology, Cerebral Spinal Fluid. In *StatPearls*. StatPearls Publishing. http://www.ncbi.nlm.nih.gov/books/NBK519007/

Trimble, C. R., Harnsberger, H. R., Castillo, M., Brant-Zawadzki, M., & Osborn, A. G. (2010). "Giant" arachnoid granulations just like CSF?: NOT!! *AJNR. American Journal of Neuroradiology*, *31*(9), 1724–1728. https://doi.org/10.3174/ajnr.A2157

Trolard, D. (1892). Les Lacunes Veineuses de la dura-mere. *J de L'anatomie*, *38*, 28–56.

Upton, M. L., & Weller, R. O. (1985). The morphology of cerebrospinal fluid drainage pathways in human arachnoid granulations. *Journal of Neurosurgery*, *63*(6), 867–875. https://doi.org/10.3171/jns.1985.63.6.0867

Vinje, V., Eklund, A., Mardal, K.-A., Rognes, M. E., & Støverud, K.-H. (2020). Intracranial pressure elevation alters CSF clearance pathways. *Fluids and Barriers of the CNS*, *17*(1), 29. https://doi.org/10.1186/s12987-020-00189-1

Wang, X.-T., Yu, H., Liu, F.-T., Zhang, C., Ma, Y.-H., Wang, J., Dong, Q., Tan, L., Wang, H., & Yu, J.-T. (2022). Associations of sleep disorders with cerebrospinal fluid α-synuclein in prodromal and early Parkinson's disease. *Journal of Neurology*, *269*(5), 2469–2478. https://doi.org/10.1007/s00415-021-10812-2

Yamada, S., Otani, T., Ii, S., Kawano, H., Nozaki, K., Wada, S., Oshima, M., & Watanabe, Y. (2023). Aging-related volume changes in the brain and cerebrospinal fluid using artificial intelligence-automated segmentation. *European Radiology*, *33*(10), 7099–7112. https://doi.org/10.1007/s00330-023-09632-x

Zou, W., Pu, T., Feng, W., Lu, M., Zheng, Y., Du, R., Xiao, M., & Hu, G. (2019). Blocking meningeal lymphatic drainage aggravates Parkinson's disease-like pathology in mice overexpressing mutated α-synuclein. *Translational Neurodegeneration*, *8*(1), 7. https://doi.org/10.1186/s40035-019-0147-y